A Velocity-Overshoot Subthreshold Current Model for Deep-Submicrometer MOSFET Devices

Wensheng Qian , Xing Zhou , Yuwen Wang and Khee Yong Lim

School of Electrical & Electronic Engineering, Nanyang Technological University, Nanyang Avenue, Singapore 639798, ewsqian@ntu.edu.sg

ABSTRACT

In this paper, a new theoretical approach to submicrometer MOSFET subthreshold current modeling is presented. The diffusion and drift currents are calculated, respectively. The effect of velocity overshoot on subthreshold current is investigated. Comparison with MEDICI simulation results verifies the model.

1 INTRODUCTION

Advances in VLSI fabrication technology drive the devices towards deep-submicrometer demensions. For many kinds of special effect such as velocity overshoot effect, short channel effect, drain-induced barrier lowering etc., submicrometer MOSFETs exhibit different characteristics compared to conventional ones. Thus unconventional approach has to be used in simulating the performance of submicrometer devices. [1,2]

Subthreshold characteristic of MOSFETs is quite important for low-voltage, low-power applications, such as when MOSFETs are used as switches in digital logic and memory applications, because the subthreshold region describes how the switch turns on and off. In the subthreshould region, the diffusion current is usually expected to be dominant, because the depletion charge is much larger than the inversion charge. But for submicrometer MOSFET, the contribution of the drift current to the total current can not be neglected, because of the stronger lateral electrical field in shorter channel device.

In this paper, an analytical model of subthreshould current of short-channel MOSFETs is presented, in which the diffusion and drift currents are calculated separately, particularly velocity overshoot and velocity saturation are taken into consideration. The calculation results of this model are compared with MEDICI data for verification.

2 MODEL DERIVATION

The schematic cross section of the MOSFET is shown in Fig.1.

The drift velocity in a homogeneous low-field v_h is given as [3]

$$v_h = -\frac{\mu E}{1+E/E_s} \qquad (|E|<|E_s|) \tag{1}$$

where E_s is the electric field at which the carrier velocity reaches saturation, μ is the low-field mobility.

The velocity overshoot is closely related to the field gradient in channel of MOSFET. The velocity in an inhomogeneous channel electric field E can be expressed approximately as [4,5]

$$v = v_h\left(1+\frac{\theta(E)}{E}\frac{dE}{dy}\right) \tag{2}$$

where $\theta(E)$ is the coefficient for the field-gradient effect which is given by

$$\theta(E) = \frac{4}{3} v_s \tau_\varepsilon \frac{2+E/E_s}{(1+E/E_s)^2}\frac{E}{E_s} \qquad (|E|<|E_s|) \tag{3}$$

where t_e is the energy relaxation time, v_s is the carrier saturation velocity which is given as

$$v_s = -\frac{\mu E_s}{2} \tag{4}$$

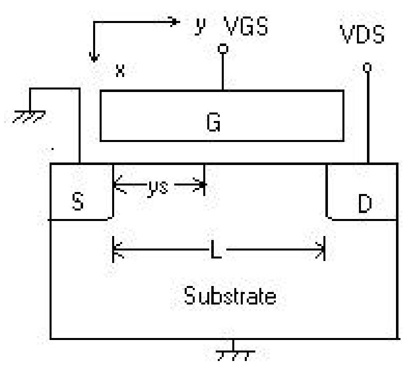

Fig.1: Schematic diagram of MOSFET device
L: the channel length of uniform doping
y_s: the point of carrier velocity saturation

The drift velocity in an inhomogeneous electric field before it reaches saturation can be expressed as

$$v(E) = -\frac{\mu E}{1+E/E_s}\left(1-\frac{2}{3}\mu\tau_\varepsilon\frac{2+E/E_s}{(1+E/E_s)^2}\frac{dE}{dy}\right) \tag{5}$$

Thus, the effective mobility μ_{eff} including overshoot effect is defined by

$$\mu_{eff} = \mu\left(1-\frac{2}{3}\mu\tau_\varepsilon\frac{2+E/E_s}{(1+E/E_s)^2}\frac{dE}{dy}\right) \tag{6}$$

The equation of channel surface potential V_s (the inversion charges are neglected in subthreshold condition) is [6]

$$\varepsilon_{Si}\frac{X_{dep}}{\eta}\frac{d^2V_s}{dy^2} + \varepsilon_{OX}\frac{V_{GS}-V_{fb}-V_s(y)}{T_{ox}} = qN_A X_{dep}/\eta \tag{7}$$

where ε_{Si} and ε_{OX} are the permittivity of Si and SiO_2, V_{GS} is the gate-source voltage, V_{fb} is the flatband voltage, T_{OX} is the gate-oxide thickness, X_{dep} is the depletion layer thickness at strong inversion with zero drain bias, which is equal to $\sqrt{4\varepsilon_{Si}\psi_F / qN_A}$, ψ_F is Fermi potential. The average depletion layer thickness at weak inversion is given as X_{dep}/η , where η is the fitting parameter. N_A is the substrate uniform doping.

The solution to (7) under the boundary conditions: $V_s(0) = V_{bi}$ and $V_s(L) = V_{DS} + V_{bi}$ (the substrate potential is taken as ground) is

$$V_s(y) = (V_{bi} + V_{DS} - V_{GS} + V_0)\frac{\sinh(y/l)}{\sinh(L/l)} + (V_{bi} - V_{GS} + V_o)\frac{\sinh[(L-y)/l]}{\sinh(L/l)} + V_{GS} - V_o \tag{8}$$

in (8), $V_o = V_{fb} + \dfrac{qN_A X_{dep} T_{OX}}{\eta\varepsilon_{OX}}$, V_{bi} is the PN junction built-in potential, l is defined as

$$l = \sqrt{\frac{\varepsilon_{Si} T_{OX} X_{dep}}{\varepsilon_{OX}\eta}} \tag{9}$$

Assuming the channel potential has a minimum at y_{min} , then

$$\frac{dV_s}{dy}\Big|_{y=y_{min}} = 0 \tag{10}$$

By solving the Poisson’s Equation, the channel surface charge Q_s can be obtained as

$$Q_s = -\frac{\sqrt{2}\varepsilon_{Si} kT}{qL_D} F[\frac{q}{KT}V_s, (\psi_n - \psi_F), \frac{n_{p0}}{P_{p0}}] \tag{11}$$

where the surface potential V_s and the quasi-Fermi potential ψ_n are the functions of the position y along the channel. And

$$L_D = (\frac{KT\varepsilon_{Si}}{P_{p0} q^2})^{1/2} \tag{12a}$$

$$\psi_F = (kT/q)\ln(N_A / n_i) \tag{12b}$$

$$F[\frac{q}{KT}V_s, (\psi_n - \psi_F), \frac{n_{p0}}{p_{p0}}] = \{e^{-\frac{q}{KT}V_s} + \frac{q}{KT}V_s - 1 + \frac{n_{p0}}{p_{p0}} e^{-\frac{q}{KT}(\psi_n - \psi_F)} [e^{\frac{q}{KT}V_s} - \frac{q}{KT}V_s e^{\frac{q}{KT}(\psi_n - \psi_F)}]\}^{1/2} \tag{12c}$$

The depletion charge Q_B is given as

$$Q_B = -(2qN_A\varepsilon_{Si}V_s)^{1/2} \tag{13}$$

In subthreshold region, from (11) and (13) the channel inversion charge Q_I can be approximately expressed as

$$Q_I = Q_S - Q_B = -\frac{\sqrt{2q\varepsilon_{Si} N_A}}{2\sqrt{V_s}} \frac{kT}{q} e^{(V_s - 2\phi_F - \delta_n)q/kT} \tag{14}$$

where $\delta_n = \psi_n - \psi_F$, which is the partial voltage drop of V_{DS} at a point in the channel.

In order to get δ_n , Gauss's law is used. The height of the Gaussian box is the depth of source and drain diffusion regions, and one of its edges is fixed at the point of y_s Then one can get the following equation[5]

$$E_s x_j - E(y)x_j - \frac{\varepsilon_{ox}}{\varepsilon_{Si}}\int_y^{y_s}\frac{V_{gs} - \delta_n(y)}{T_{ox}}dy = -\frac{q(N_A + N_I)}{\varepsilon_{Si}} x_j (y_s - y) \tag{15}$$

where N_I is the bulk density of inversion charge, E(y) is the channel lateral electric field, and E_s is the electric field at which carrier velocity saturates. Differentiating (15) with respect to y, one obtains

$$\frac{dE(y)}{dy} x_j - \frac{\varepsilon_{ox}}{\varepsilon_{Si}}\frac{V_{GS} - \delta_n(y)}{T_{ox}} = -\frac{q(N_A + N_I)}{\varepsilon_{Si}} x_j \tag{16}$$

When $y = y_s$, and the channel lateral electric field near source end is assumed to increase linearly in order to simplify (15) and (16), [5] (16) becomes

$$\frac{E_s}{y_c} x_j - \frac{\varepsilon_{ox}}{\varepsilon_{Si}}\frac{V_{GS} - \delta_n(y_s)}{T_{ox}} = -\frac{q(N_A + N_I)}{\varepsilon_{Si}} x_j \tag{17}$$

subtracting (17) from (16), one obtains

$$-\frac{dE(y)}{dy} = \frac{\delta_n(y) - \delta_n(y_s)}{\lambda^2} - \frac{E_s}{y_s} \tag{18}$$

where

$$\lambda = \sqrt{\frac{\varepsilon_{Si}}{\varepsilon_{ox}} T_{ox} x_j} \tag{18a}$$

Equation (18) can be rewritten as

$$\frac{d^2\delta_n(y)}{dy^2} = \frac{\delta_n(y) - \delta_n(y_s)}{\lambda^2} - \frac{E_s}{y_s} \tag{19}$$

Apparently, the boundary conditions of (19) are as follows

$$1.\quad \frac{d\delta_n(y)}{dy}\Big|_{y=y_s} = -E_s \tag{19a}$$

$$2.\quad \delta_n(0) = 0 \tag{19b}$$

$$3.\quad \delta_n(L) = V_{DS} \tag{19c}$$

With these boundary conditions, (19) can be solved as

$$\delta_n(y) = ae^{y/\lambda} + be^{-y/\lambda} + \frac{E_s\lambda^2}{y_s} + \delta_n(y_s) \tag{20}$$

where

$$a = \frac{V_{DS}}{e^{L/\lambda} - 1} + \frac{\lambda E_s (1 - e^{-L/\lambda})}{e^{(L-y_s)/\lambda} - e^{-y_s/\lambda} - e^{y_s/\lambda} + e^{(y_s - L)/\lambda} - V_{DS} e^{y_s/\lambda}} \tag{21}$$

$$b = \frac{\lambda E_s (e^{L/\lambda} - 1)}{e^{(L-y_s)/\lambda} - e^{-y_s/\lambda} - e^{y_s/\lambda} + e^{(y_s - L)/\lambda} - V_{DS} e^{y_s/\lambda}} \tag{22}$$

Combining (19a), (20), (21), (22), y_s can be obtained. From (19b) and (20), $\delta_n(y_s)$ has the following relation

$$\delta_n(y_s) = -\frac{E_s\lambda^2}{y_s} - a - b \qquad (23)$$

With the expression of inversion charge, the drift and diffusion currents of a MOSFET can be written as

$$\begin{aligned} I_{drif}(y) &= -WQ_I(y)v(y) \\ &= W\left[\frac{\sqrt{2q\varepsilon_{Si}N_A}}{2\sqrt{V_s(y)}}\phi_t e^{[V_s(y)-2\phi_F-\psi_n(y)]/\phi_t}\right]\times\frac{\mu_{eff}E_s(y)}{1+E_s(y)/E_c} \end{aligned} \qquad (24)$$

$$I_{diff} = -D_n W\frac{dQ_I(y)}{dy} = -KT\mu_{eff}W\frac{dQ_I(y)}{dy} \qquad (25)$$

where

$$\begin{aligned} \frac{dQ_I(y)}{dy} &= -\frac{\sqrt{2q\varepsilon_{Si}N_A}}{2\sqrt{V_s(y)}}e^{[V_s(y)-2\phi_F-\delta_n(y)]/\phi_t}\left[\frac{dV_s(y)}{dy}-\frac{d\delta_n(y)}{dy}\right] \\ &+\frac{\sqrt{2q\varepsilon_{Si}N_A}}{4[V_s(y)]^{3/2}}\phi_t e^{[V_s(y)-2\phi_F-\delta_n(y)]/\phi_t}\frac{dV_s(y)}{dy} \end{aligned} \qquad (26)$$

$$\begin{aligned} \frac{dV_s(y)}{dy} &= \frac{(V_{bi}+V_{DS}-V_{SL})}{l}\frac{\cosh(y/l)}{\sinh(L/l)} \\ &-\frac{(V_{bi}-V_{SL})}{l}\frac{\cosh(\frac{L-y}{l})}{\sinh(L/l)} \end{aligned} \qquad (27)$$

$$\frac{d\delta_n(y)}{dy} = \frac{a}{\lambda}e^{y/\lambda} - \frac{b}{\lambda}e^{-y/\lambda} \qquad (28)$$

Integrating (24) and (25) from 0 to y_s, the channel drift and diffusion currents can be easily obtained. The device drain current is the sum of the drift and diffusion currents.

Because the effect of channel length modulation is apparent in deep-submicrometer devices, the effective channel length in [7] is applied to replace of the channel length (L) in the above equations:

$$L_{eff} = \exp(qV_{s\min}/KT)\int_0^L \exp[-qV_s(y)/KT]dy \qquad (29)$$

3 RESULTS AND DISCUSSION

The physical and device structure parameters used in the simulation are listed in Table 1.

In order to observe the distribution of surface potential along the channel, the calculated surface potentials for three channel lengths (0.25μm, 0.5μm and 1μm) at V_{DS}=4V and V_{GS}=0.3V are plotted together in Fig2. It is apparent that the surface potential is almost constant for long channel, but has a large variation in short channel devices. This shows that it is necessary to use various surface potentials for deep-submicrometer device simulation.

Fig.3 (a, b) shows the of calculated drain current vs gate voltage at V_{DS}=2V, 4V, and compares with MEDICI simulation. The parameter η (=1) in the model is determined as 1 by fitting to the MEDICI data at V_{DS}=4V and V_{GS}=0.1V. The calculated results agree well with MEDICI in subthreshould region (Vth=0.37V) at different V_{DS}. The reason for the increasing discrepancy with MEDICI results above Vg_S=0.4V is that the model does not include inversion charge. However this should not influence the device subthreshold performance.

To clarify the carrier velocity overshoot effect on device subthreshold characteristics, we compare the calculated drain currents with those ignoring the overshoot effect at V_{DS}=2V and 4V, as shown in Fig.4 (a, b). Without overshoot , the effective mobility in high field is replaced with the low field mobility. At V_{DS}=2V, the difference between the drain currents with and without overshoot is quite small. But when V_{DS} becomes larger, overshoot effect becomes very obvious. At low drain bias, the lateral electric field near the source is small, and the velocity overshoot effect is not significant. At large drain voltage, the electric field near source increases, the carrier can gain much more energy in the channel, and velocity overshoot becomes more apparent. High lateral electric field in the channel is the basic factor of overshoot effect. Both short channel and high drain bias are the conditions under which this effect appears.

4 CONCLUSIONS

This paper presents a new physics-based subthreshold current model for deep-submicrometer MOSFETs. In the model, an effective mobility including carrier velocity overshoot is used to replace the low electric field mobility. The simulation results show that overshoot effect is very important at short channel and high drain bias. Accurate channel surface potential model is essential for drain current simulation because it is no longer a constant in short channel. Gauss Law is adopted to calculate the surface potential, partial voltage drop of drain bias and the quasi-Fermi level at every point in the channel. The weak inversion charge model is developed by solving Poisson equation involving the expressions of surface potential and quasi-Fermi level. Drift current can not be neglected in short channel devices, especially at high drain voltages. The calculated results of this model agrees well with numerical data in the subthreshold region.

Parameter	**Value**
Energy relaxation time τ_ε	0.17ps
Carrier velocity saturation Electric field $\lvert E_s \rvert$	1×10^6 V / m
Gate length L_g	0.39 μm
Depth of source and drain diffusion x_j	60nm
Uniform substrate doping N_A	$3\times10^{17}\ cm^{-3}$
Uniform doping channel length L	0.25μm
Thickness of gate oxide layer T_{ox}	4.5nm

Table 1: Physical[5] and Device Structure Parameters

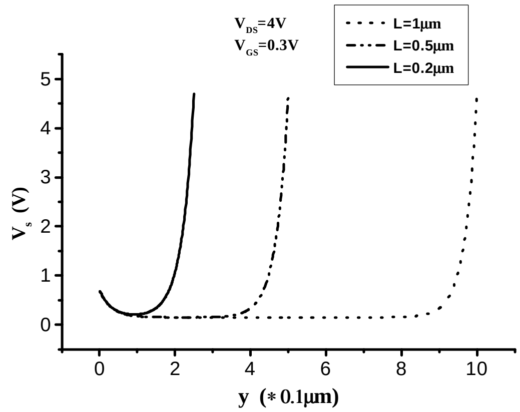

Fig.2: Channel surface potential vs. channel position y for three gate lengths

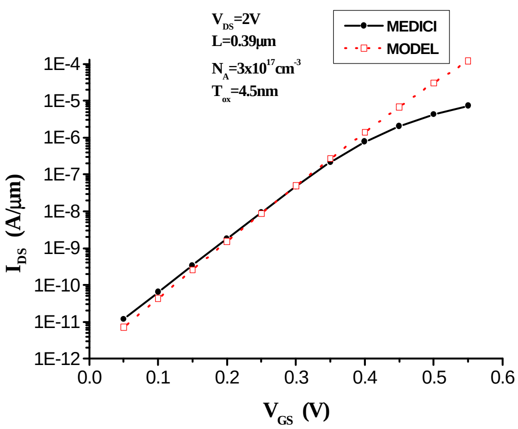

(a)

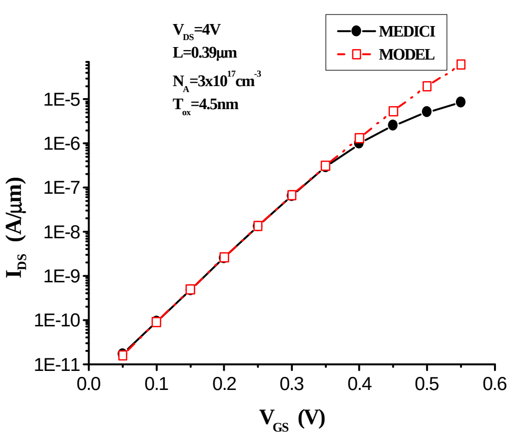

(b)

Fig.3: Calculated and MEDICI simulated drain current I_{DS} as a function of gate voltage V_{GS}
(a): V_{DS}=2V (b): V_{DS}=4V

REFERENCES

[1] Sheng-Lyang Jang and Mam-Chun Hu, "An Analytical Drain Current Model for Submicrometer.

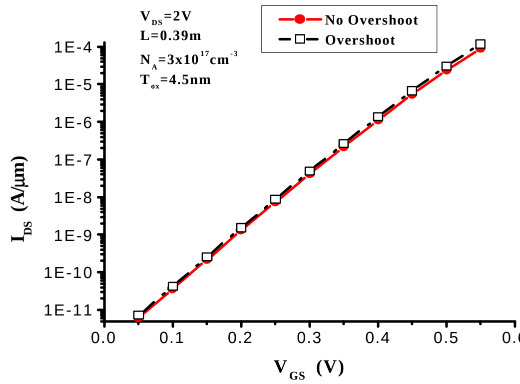

(a)

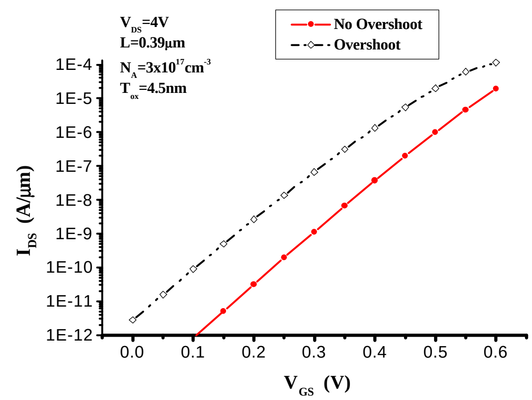

(b)

Fig.4: Calculated drain current I_{DS} as a function of gate voltage V_{GS} with or without overshoot
(a): V_{DS}=2V b: V_{DS}=4V

and Deep Submicrometer MOSFET", IEEE Trans. Electron Devices, 44(11), pp. 1896-1902, 1996.

[2] Soonwon Hong and Kwyro Lee, "Extraction of Metal -lurgical Effective Channel Length in LDD MOSFETs", IEEE Trans. Electron Devices, 42(8), pp. 1461-1466, 1995

[3] B. Hoefflinger, H. Sibbert, and G. Zimmer, "Model and performance of hot-electron MOS transistors for VLSI", IEEE Trans. Electron Devices, vol. ED-26, pp. 513-520, 1979.

[4] P. J. Price, "On the flow equation in device simulation", J Appl. Phys., vol.63, pp. 4718-4722, 1988.

[5] Ken'ichiro Sonoda, Kenji Taniguchi, and Chihiro Hamaguchi, "Analytical Device Model for Submicrometer MOFETs", IEEE Trans. Electron Devices, 38(12), pp. 2662-2668, 1991.

[6] Zhi-Hong Liu, Chenming Hu, Jian-Hui Huang, Tung-Yi Chan, Min-Chie Jeng, Ping K. Ko, Y. C. Cheng, "Threshold Voltage Model for Deep-Submicrometer MOSFETs", IEEE Trans. Electron Devices, 40(1), pp. 86-93, 1993.

[7] G. W. Taylor, "Subthreshold conduction in MOSFETs", IEEE. Trans. Electron Devices, vol. ED-25, pp. 337-350, 1978.